Hour-ahead Forecasting of Photovoltaic Power Output based on Hidden Markov Model and Genetic Algorithm

Victor Eniola*,**, Tawat Suriwong*‡, Chatchai Sirisamphanwong***, Kasamsuk Ungchittrakool****

* School of Renewable Energy and Smart Grid Technology, Naresuan University, Phitsanulok 65000, Thailand

** Energy Commission of Nigeria, Abuja 900211, Nigeria

*** Department of Physics, Faculty of Science, Naresuan University, Phitsanulok 65000, Thailand

**** Department of Mathematics, Faculty of Science, Naresuan University, Phitsanulok 65000, Thailand

(enilav01@yahoo.com, tawats@nu.ac.th, chatchaisi@nu.ac.th, kasamsuku@nu.ac.th)

‡Corresponding Author; Tawat Suriwong, School of Renewable Energy and Smart Grid Technology, Naresuan University, Phitsanulok 65000, Thailand, Tel: +66 5596 3180,

Fax: +066 5596 3182, tawats@nu.ac.th

Received: 01.04.2019 Accepted: 30.04.2019

Abstract- It is well known that the variability in PV power output is primarily owing to fluctuations in radiation received by the solar panels. Forecasting in the short-term horizon particularly is very crucial to power quality and power schedules such as load drop or gain, and power dispatch planning. This study details an innovative method based on ordinary model (Hidden Markov Model, HMM) and HMM optimized with Genetic Algorithm (GA) for hour-ahead forecasting of the power output (P_o) of a 1.2 kW PV system. Solar irradiance, module temperature acquired by mathematical modelling and wind speed were used as initial forecast data. The model testing and validation was built on the computation of normalized Root Mean Square Error (nRMSE). As the results, GA-optimized HMM is able to forecast P_o an hour-ahead with low nRMSE than HMM under clear sky day (CSD) condition. However, the abnormalities of the forecasting model resulting from instantaneous fluctuations in solar irradiance under cloudy day (CD) condition were decreased with correction factor (ξ). It was deduced that if the average change in the absolute value of solar irradiance ($|\overline{\Delta G_s}|$) is more than 128% and 90% in the morning and evening times respectively, the GA-optimized forecasting model with or without ξ presents average nRMSE of 2.33%. Therefore, HMM+GA gives more accurate P_o forecast for CSDs whereas HMM+GA+ξ presents the best P_o for CDs, supporting the consideration of the proposed forecast model as a good technique for hour-ahead power output forecasting of PV system.

Keywords Forecasting, Photovoltaic, Power, Hidden Markov Model (HMM), Genetic Algorithm.

Nomenclature

PV	photovoltaic	MAPE	mean absolute percentage error
HMM	hidden Markov model	G_s	solar irradiance
GA	genetic algorithm	$\|\overline{\Delta G_s}\|$	average percentage change in absolute value of solar irradiance
kW	kilowatts		
nRMSE	normalized root mean square error		

$\lvert\overline{\Delta G_s}\rvert_m$	average percentage change in absolute value of solar irradiance in the morning
$\lvert\overline{\Delta G_s}\rvert_e$	average percentage change in absolute value of solar irradiance in the evening
ξ	correction factor
NWP	numerical weather prediction
ANN	artificial neural network
ARIMA	autoregressive integrated moving average
ELM	extreme learning machine
SVR	support vector regression
GRP	Gaussian process regression
T_m	module temperature
T_{amb}	ambient temperature
w	wind speed
P_o	power output
VA	Viterbi algorithm
η	module efficiency
A_m	module area
α	temperature coefficient (power)
P_{rated}	rated power of PV system
P_a	actual power
P_f	forecasted power
n	number of time periods for power production
P_{act}	actual power output
P_{HMM}	HMM power output
P_{opt}	optimized power output
CSD	clear sky day
CD	cloudy day
PSO	particle swarm optimization
MRE	mean relative error
RBF	radial basis function
FNN	feedforward neural network

1. Introduction

With respect to climate issues and global warming, various incentives and energy guidelines that can advance the penetration of renewables have been orchestrated in many countries [1]. It is possible to operate 100% renewable energy-based electric power grid in 2050 [2]. Among the renewable resources, solar power is one of the technologies that is being considered recently in view of its benefits such as inexhaustibility and near-zero pollution. In recent years, mean growth of Photovoltaic (PV) system is up to 30% annually [3]. PV power is a promising complement for the dwindling fossil fuel-based system [4, 5]. Alongside with the diminishing prices of PV modules, it is anticipated that the PV power supply to energy systems and the modern electric power would grow further. To meet the world's energy need, PV power is a viable solution. However, the PV technology is confronted still with some difficulties particularly for high supply in which intermittency and discontinuity are pronounced [6]. Meteorological parameters influence the PV power plant production capacity. The variability in PV power output is primarily owing to fluctuations in radiation received by the solar panels. This inherent unpredictability of PV power at higher supply to the grid gives complications relating to conveyable generation, reserve costs, power quality and overall dependability of the grid [7]. As such, models with high forecast accuracy are essential for various forecast horizons related to law, scheduling, unit commitment and transmission [8]. Forecast horizon can be classified as either short-term, medium-term or long-term. With short-term forecasting, intermittency problem associated with PV based power production as well as power quality issues can be addressed. Particularly, short-term forecasting is very crucial to power schedules such as load drop or gain, and power dispatch planning. It affords improvement in power system control and reliability, increases the penetration of PV power technology, enhances energy planning and management. With short-term forecasting, energy price can be determined beforehand. Forecast models are characterized into three namely: physical models; statistical techniques and hybrid approaches. Physical methods, such as Numerical Weather Prediction (NWP) model, explains solar energy to electrical power conversion. On daily basis, power production can be predicted with physical methods by utilizing a given day's probable weather conditions. Alternatively, statistical approaches such as Artificial Neural Network (ANN) based on persistent notion or probabilistic time series model, for example, an Autoregressive Integrated Moving Average (ARIMA), classically depend on machine learning processes. With this method, renewable energy-based power prediction can be implemented using historical training dataset which can be of any size. However, it requires striking a balance between training dataset size and model sensitivity. The larger the training dataset, the better the model accuracy with respect to long-term trend study. When two or more physical and/or statistical methods are integrated, the resulting combination is referred to as a hybrid model. Such amalgamation has the advantage of outweighing the drawbacks associated with standalone approach and finally improves the forecast [9].

Hidden Markov Model (HMM) is a model in which a sequence of states generates a sequence of observation or emission, though the states sequence the model passed through to produce the emission is not known. The

attribute *hidden* signifies the sequence of states the model went through, and not to the model parameters. Even if these parameters are exactly known, the model is still an HMM. The model has determinate internal states that generate a set of external emissions. The changes in the internal states are not observable to an external examiner. A unique Markov property is that the present state is always dependent on the immediately preceding state only. Analysis of HMM seeks to recover the sequence of states from the observed data. This model hinges on the estimation of transition and emission probabilities. Short term hour-ahead prediction of PV power is very crucial to power quality and power schedules such as load drop or gain, and power dispatch planning. In the prediction of varying power supply, ANN has been applied severally with an acceptable level of success. Nevertheless, it requires more robust training dataset and the selection of HMM is informed by some other considerations such as its adaptability; richness in mathematical structure and ability to describe data more accurately with an optimal increase in the number of discrete states [10, 11].

PV power output forecast has been carried out with several methods such as neural networks [12-14], grey theory [15, 16], cloud modelling [17], random forests [8], Support Vector Regression (SVR) [18], Gaussian Process Regression (GPR) [19] and hybrid approach [20, 21]. PV power output has also been forecasted based on Markov processes [15]. Recently, efforts have been made to predict streamflow for water resource management [10], prediction of solar irradiance [22] using HMM. Nevertheless, there is need to improve the forecasting capability of the model.

In this study, therefore, a time series mathematical forecasting model based on ordinary model (HMM) and HMM optimized with Genetic Algorithm (GA); expressed as HMM+GA, is proposed to predict hour-ahead power output of a 1.2 kW PV system. GA makes use of a population whose size is fixed and comprising individual distinct probable solutions to a given problem, which evolve in time. It applies the selection, recombination (crossover) and mutation operators to exclude the poorest solutions and generate new results from the selected current ones. To smoothen abnormalities resulting from abrupt changes in solar irradiance (G_s), the correction factor (ξ) is required to adapt the HMM and HMM+GA models. The key contribution of our study is the comparison of HMM and HMM+GA forecasting models in PV power prediction. The effectiveness of the integration of GA and model adaptation with ξ to improve the forecast accuracy of the model is also discussed.

2. Methodology

The power output (P_o) of the 1.2 kW thin-film silicon modules installed at the School of Renewable Energy and Smart Grid Technology (SGtech), Naresuan University, Thailand, as shown in Fig.1, is forecasted based on historical data of G_s, ambient temperature (T_{amb}) and wind speed (w). Figure 2 presents the flowchart of the PV power output forecast process. First, the data is filtered to 1-hr time resolution followed by data refinement to compensate for missing or negative data points by replacing them with their monthly averages. In order to avoid irrational error value at the validation step, the dataset was preprocessed to eliminate zero-value data occurring at early hours and night times. Subsequently, the dataset is divided into two quotas. About 95% of the dataset is used for training while the remaining is used for forecasting model validation. To consider very short-term forecasting, G_s and module temperature (T_m) are the best parameters to precisely forecast rapid PV energy variations due to cloud cover and T_m significant effect on voltage which invariably affects the P_o of the PV system [17, 23]. In the present study, the T_m is determined from T_{amb} using mathematical transformation as expressed in Eq. (1) [17, 24].

$$T_m = 0.943T_{amb} + 0.028G_s - 1.528w + 4.3 \quad (1)$$

Fig. 1. 1.2 kW PV system at SGtech, Phitsanulok, Thailand.

Table 1. Categorization of G_s

G_s (W/m^2)	State	Class
≤ 200	1	very cloudy
≤ 400	2	cloudy
≤ 600	3	partial cloud
≤ 800	4	clear sky
> 800	5	very clea sky

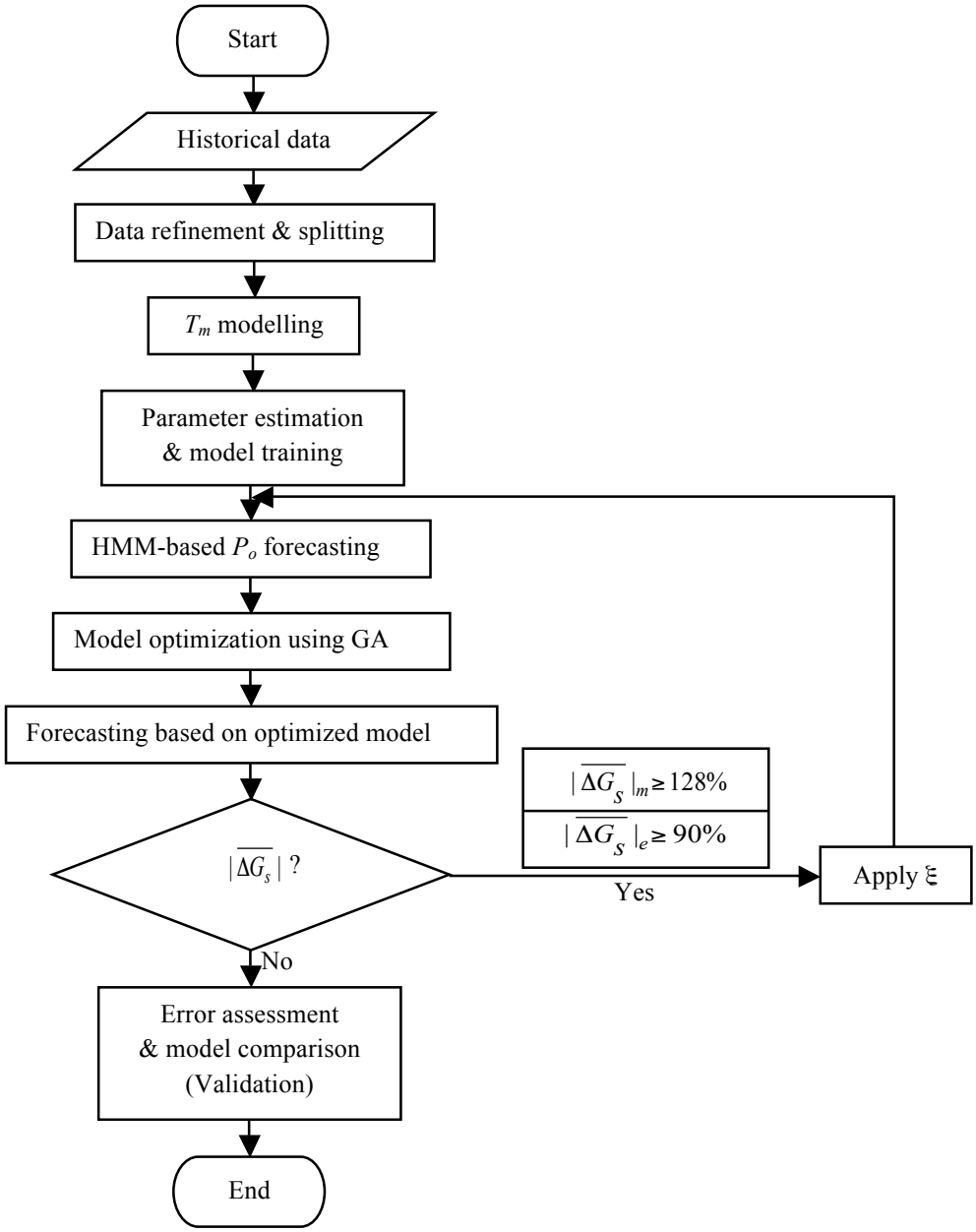

Fig. 2. Flowchart of PV power output forecast process.

In estimating parameters and model training, the use of HMM necessitates the determination of the likelihood of sequence of observations, predicting the next observation in the sequence of observations and finding the most likely underlying explanation of the sequence of observation. The solutions to these problems require the forward part of the forward-backward algorithm, Viterbi Algorithm (VA) and the Baum-Welch algorithm [11, 25]. For model development, G_s is categorized into five different states according to the following rules; as shown in Table 1. The state classification corresponds to very cloudy, cloudy, partial cloud, clear sky and very clear sky. On the other hand, the observations are also grouped into three levels equivalent to low, moderate and high generations. The latent variables of the HMM are discrete and express to a Markov chain. Supervised training is implemented by equating outputs to states and inputs to observations. The model learned from input-output relationship and makes predictions based on models of observed data. To predict with HMM, the training data is sequenced and the transition matrix with other model parameters are estimated. After 500 number of iterations of the Baum-Welch algorithm was specified in training the model, the state transition probability distribution matrix A is as given:

$$A = \begin{bmatrix} 0.514 & 0 & 0 & 0.470 & 0.016 \\ 0.487 & 0.500 & 0 & 0.013 & 0 \\ 0 & 0.569 & 0.066 & 0 & 0.365 \\ 0 & 0 & 0.504 & 0.402 & 0.094 \\ 0 & 0.038 & 0.024 & 0.376 & 0.562 \end{bmatrix} \quad (2)$$

With five number of discrete states, A is of the order 5 × 5. Element a_{ij} represents the probability distribution of transitioning from state i to j. Thus, $a_{ij} \geq 0$ and $\sum_{1}^{N} a_{ij} = 1$, for $1 \leq i \leq N$. Viterbi decoding gives the highest probable state sequence that is employed to predict the next hour power output. The P_o formula which the model relies upon for prediction is expressed in Eq. (3) [26].

$$P_o = \eta A_m G_s \left[1 - \alpha (T_m - 25)\right] \quad (3)$$

To obtain P_o at time t +1, G_s and T_m at time t are initialized and passed unto the forecast model. The power forecasting has been implemented using HMM toolbox™, as determined in the HMM-based P_o forecasting step.

Parameter optimization and model improvement are built on GA. All input parameters are initialized and the fitness function, expressed as the sum of square of the deviation between actual and fitted values, is created. To optimize this function using GA, a function handle is passed to the fitness function together with the number of variables in the problem. To also ensure that GA scrutinizes the region of relevance, preselected upper and lower bounds are passed as arguments following number of variables. When the fitness value becomes less than the function tolerance, the optimization process is terminated. Optimized parameters are adopted for the modification of the HMM, forming a sort of GA-optimized HMM. At the validation step, abnormalities observed to have resulted from instantaneous changes in solar irradiance are smoothened using ξ. If the average change in the absolute value of solar irradiance ($|\overline{\Delta G_s}|$) is more than 128% in the morning, and/or if $|\overline{\Delta G_s}|$ in the evening time exceeds 90%; then the adoption of ξ becomes crucial. However, GA optimization process is considered non-recursive in the case for which the adoption of ξ is necessary. The computation of ξ is based on interior-point algorithm. This algorithm requires a fitness assignment and a constraint set by error definition, bounds whose upper value is set at the corresponding actual power output (P_{act}) and parameter initialization.

The results of the ordinary model and proposed optimized model are comparatively analyzed in the validation process, using the testing and validation dataset. The study utilized statistical methods involving normalized Root Mean Square Error (nRMSE) and Mean Absolute Percentage Error (MAPE), which are computed as follows:

$$nRMSE = \frac{1}{P_{rated}} \sqrt{\frac{1}{n} \sum_{i}^{n} (P_{a,i} - P_{f,i})^2} \quad (4)$$

$$MAPE = 100 \times \frac{1}{n} \sum_{i}^{n} \frac{|P_{a,i} - P_{f,i}|}{P_{a,i}} \quad (5)$$

Both methods are measures to compare the forecasted P_o with the P_{act} value. Such computations provide an insight into the degree of reliability of the forecast model. An efficient forecast model is expected to present a low value of nRMSE or MAPE.

3. Results and Discussion

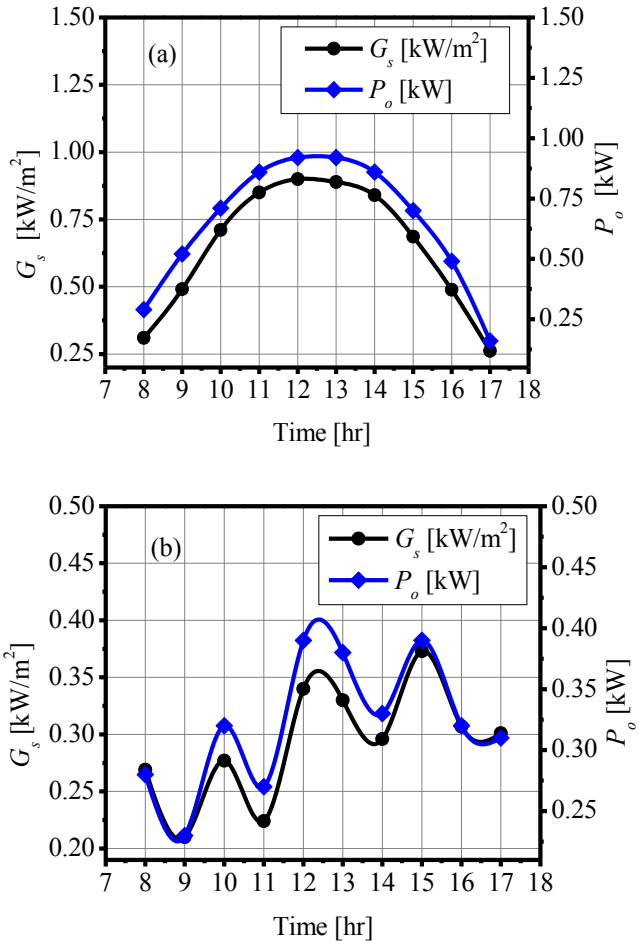

Fig. 3. Time dependence of G_s and P_o correlation for a clear (a) and cloudy (b) sky condition.

Figure 3 presents the G_s and P_o of the 1.2 kW PV system correlation for clear and cloudy sky. It is well known that the P_o increases with increasing G_s. In Fig.3a, it is observed that the P_o and G_s profiles are symmetrically distributed over time due to the typical nature of the Clear Sky Day (CSD). The highest P_o is about 83% rated power of the PV system (P_{rated}) from 12:00 to 13:00. On the other hand, both the P_o and G_s present the instantaneous change along the day (Fig.3b). However, regardless of the sky condition under consideration, P_o maintains a profile analogous to that of G_s. This similarity is indicative of the strong correlation between both parameters.

Figure 4a presents the results of P_o model validation of 09.04.2018 using ordinary model (HMM) and optimized model (HMM+GA). Power output forecasted with HMM (P_{HMM}) is not close to the P_{act}, particularly between 11:00 and 15:00. In order to improve the P_o forecasting close to the P_{act}, the HMM is optimized with GA. So, the power output determined with GA-integrated HMM, expressed as

P_{opt}, almost match with the P_{act}. To consider the error of HMM and HMM+GA (Fig.4b), the values of $nRMSE_{opt}$ are almost lower than that of $nRMSE_{HMM}$. The HMM is observed to over-forecast the data points with an ensemble nRMSE of 5.36%, whereas the ensemble nRMSE of GA-integrated HMM is reduced to 2.55%.

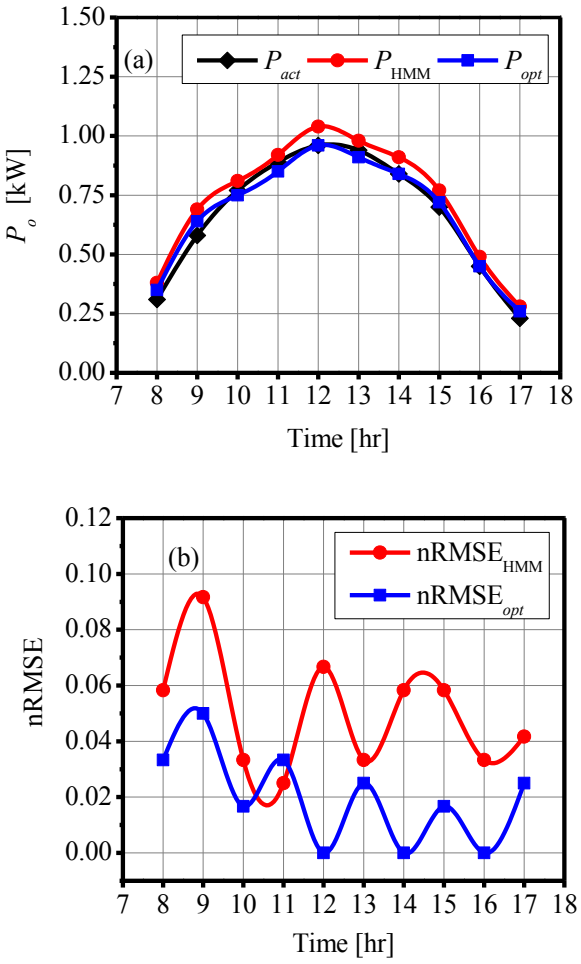

Fig. 4. P_o forecast and nRMSE of models on 09.04.2018 using HMM and HMM+GA.

The HMM and HMM+GA P_o forecast validation on 15.04.2018, is as shown in Fig.5a. The P_o output forecasting using HMM is higher above P_{act}, particularly between 10:00 and 15:00. The over-forecast of the HMM is reduced with the HMM+GA model which forecasts the P_{opt} to match almost with the P_{act}. Error consideration based on nRMSE (Fig.5b) shows that $nRMSE_{opt}$ values are well below those of $nRMSE_{HMM}$. The HMM gives a maximum nRMSE of about 9% between 10:00 and 11:00, whereas the optimized model presents a maximum nRMSE value nearly 3% at around the hours of 12:00 and 16:00. The ensemble $nRMSE_{HMM}$ of 6.27% as against 1.57% for $nRMSE_{opt}$ further explains the overshooting nature of the HMM.

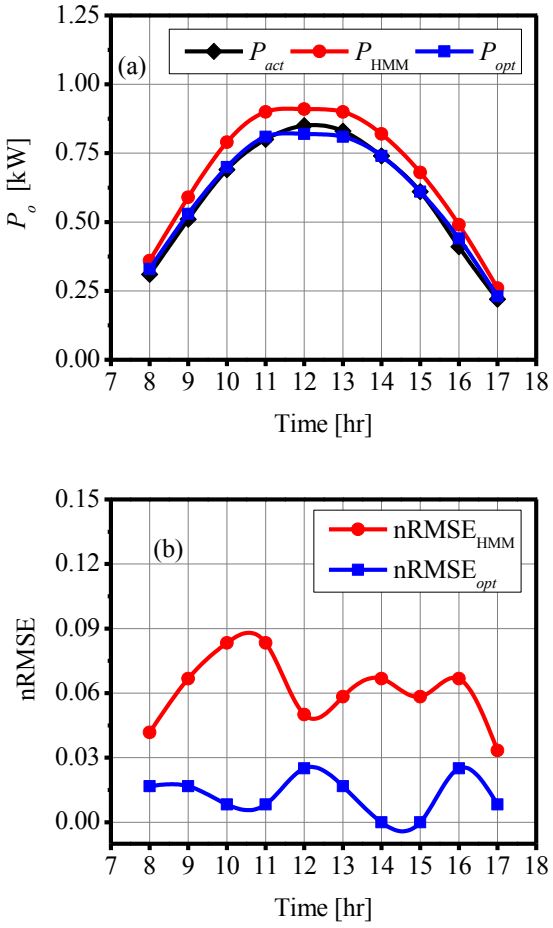

Fig. 5. P_o forecast and nRMSE of models on 15.04.2018 using HMM and HMM+GA.

In a much similar manner, the HMM+GA model predicted more accurately than P_{HMM} for the day 23.04.2018, as shown in Fig.6a. The power overshoot of the P_{HMM} escalated at 13:00 hour, but the predictions with P_{opt} is however overlapping with P_{act} values. The improvement in P_o forecasting is attributable to the integration of GA with HMM. Considering the error of both forecast models, the values of $nRMSE_{opt}$ are lower than those of $nRMSE_{HMM}$, according to Fig.6b. The $nRMSE_{HMM}$ corresponding to the maximum power overshoot is about 9%, whereas the peak of the $nRMSE_{opt}$ is lower than 4%. With P_{opt}, ensemble nRMSE decreased considerably from 6.33% to 1.77%. Computational analysis reveals that the HMM optimized with GA is capable of improving the reliability of the P_o forecasting by 4.56%.

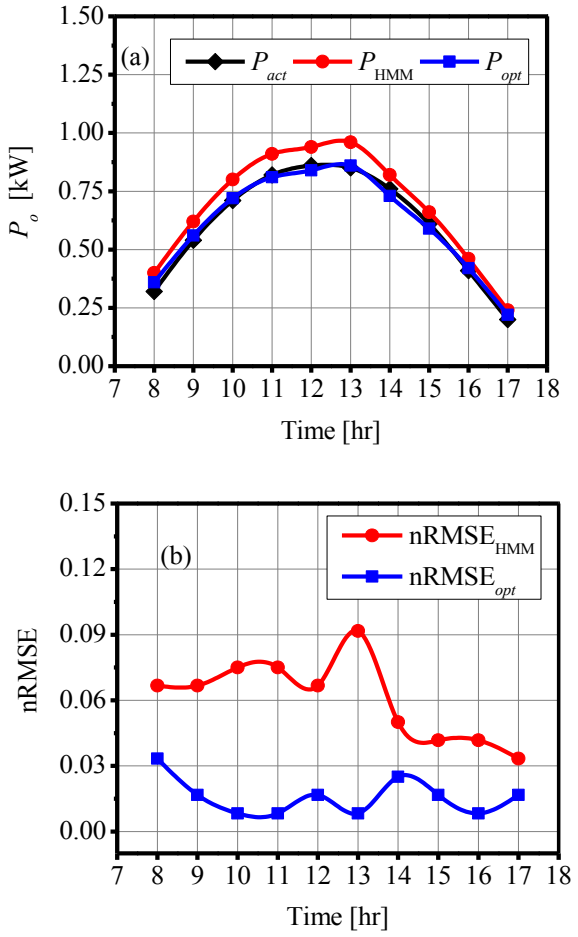

Fig. 6. P_o forecast and nRMSE of models on 23.04.2018 using HMM and HMM+GA.

Figure 7a presents the results of P_o model validation of the day 30.04.2018 based on HMM and HMM+GA. It is observed that the P_{act} fluctuates as a result of the cloudy sky condition. The P_{opt} is closer to P_{act} than P_{HMM} over the entire day. However, P_{HMM} and P_{opt} do not approach P_{act} primarily due to the influence of sudden changes in G_s at 8:00 and 17:00 hours. According to their nRMSE curve (Fig.7b), both nRMSEs present the highest values. Additionally, nRMSE$_{opt}$ and nRMSE$_{HMM}$ have the highest values of about 26-28% and 32-35% respectively. It indicates that HMM and HMM+GA models have a limitation for instantaneous changes in G_s. To rectify abnormality, correction factor (ξ) was adopted based on HMM+ξ and HMM+GA+ξ with the criteria outlined in the methodology section. The ξ plays a crucial role on Cloudy Day (CD) when the $|\overline{\Delta G_s}|$ is more than 128% in the morning, and/or if $|\overline{\Delta G_s}|$ in the evening time exceeds 90%. The computed values of ξ used to smoothen the data at 8:00 and 17:00 hours were 0.40 and 0.24 respectively. Sequel to the use of ξ, both P_{HMM} and P_{opt} present more reasonable P_o curves in Fig.8a. Considering the influence ξ-adapted HMM and ξ-adapted HMM+GA on the nRMSE (Fig.8b), it can be observed that nRMSE$_{HMM}$ and nRMSE$_{opt}$ in the hours of 8:00 and 17:00 reduced close to 3% and zero respectively. The reduced peaks of nRMSE$_{opt}$ and nRMSE$_{HMM}$ coupled with their respective ensemble nRMSE values decreasing to 5.61% and 4.29% further strengthen the correctional strength and significance of ξ. To compare HMM and HMM+GA adapted with and without ξ (Fig.7 and Fig.8), the abnormalities and nRMSE are significantly reduced with the use of ξ and the values of nRMSE of ξ-adapted HMM and HMM+GA are less fluctuating than without the ξ.

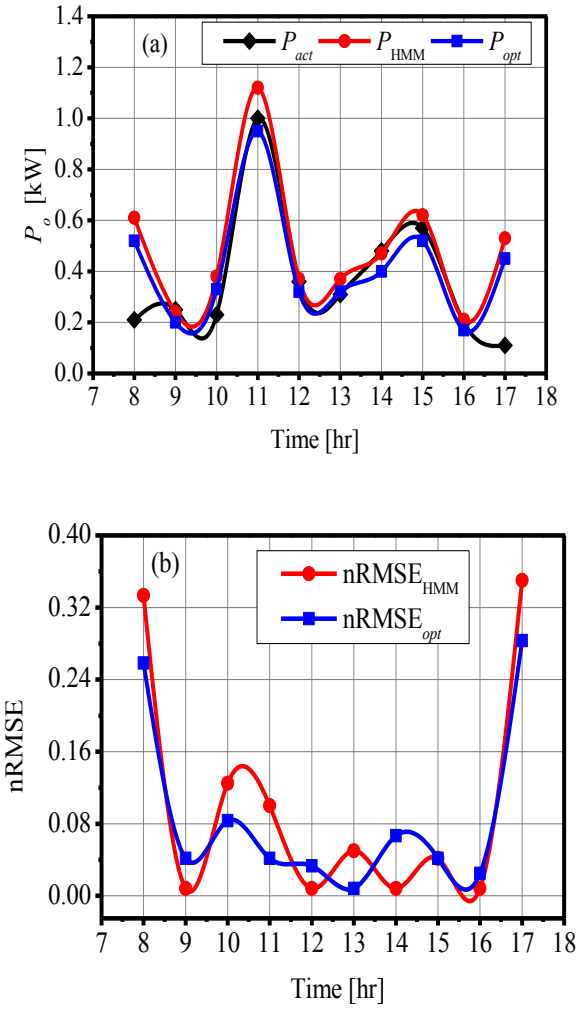

Fig. 7. P_o forecast and nRMSE of models on 30.04.2018 using HMM and HMM+GA.

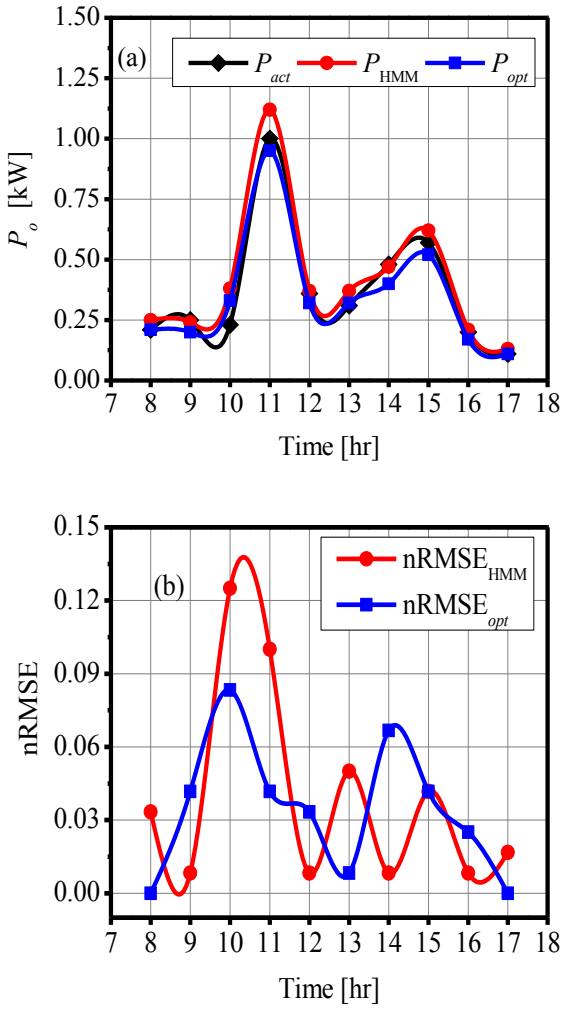

Fig. 8. P_o forecast and nRMSE of models on 30.04.2018 using HMM+ξ and HMM+GA+ξ.

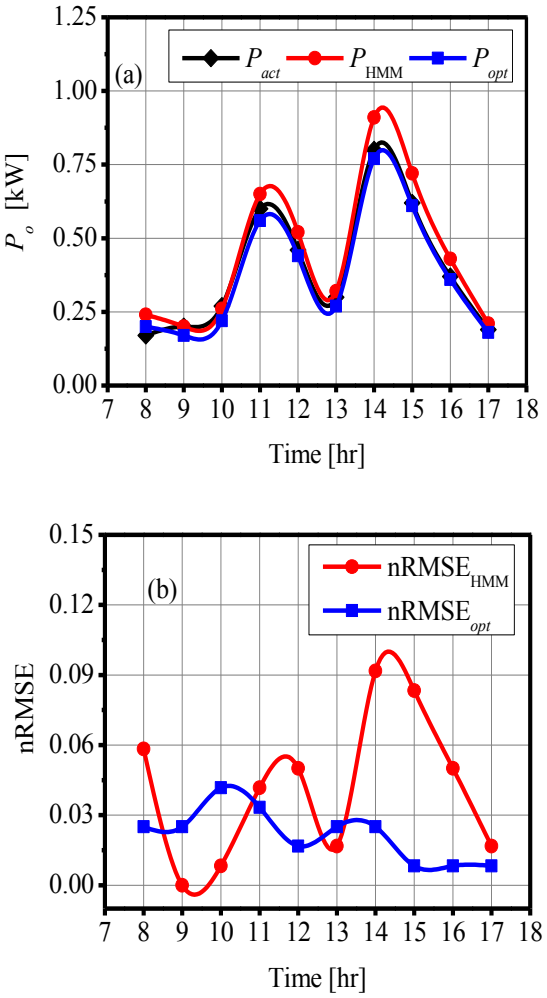

Fig. 9. P_o forecast and nRMSE of models on 25.03.2018 using HMM+ξ and HMM+GA+ξ.

Figure 9a presents the result comparison of P_o forecast models for the day 25.03.2018 using HMM+ξ and HMM+GA+ξ on cloudy sky condition. The computed value of ξ used to adapt the abnormalities occurring at 8.00 and 9.00 is 0.33. P_o forecasted with HMM+ξ presents overshoots noticeably around 11:00 and 14:00. In order to improve the P_o close to the P_{act}, P_{opt} was predicted based on HMM+GA+ξ model; which is perceived to forecast P_o more accurately. To consider the forecast error (Fig.9b), the ensemble nRMSE$_{opt}$ values of 2.42% for the HMM+GA+ξ is lower than the 5.11% nRMSE$_{HMM}$ of the HMM+ξ; especially the value of HMM+GA+ξ relatively maintains a range around 1-4%.

Figure 10a presents the results of P_o forecast for the day 26.06.2018 based on cloudy sky condition using HMM+ξ and HMM+GA+ξ models. The computed value of ξ used to fine-tune the abnormalities occurring at 8:00 is 0.41 and those occurring from 15:00 – 17:00 are adjusted with ξ = 0.35. P_{HMM} and P_{opt} with both models present good agreement with P_{act} along the entire day. The improvement in power output prediction with HMM+GA+ξ can be perceived by considering the nRMSE curves shown in Fig.10b. Fortunately, the curve of nRMSE$_{HMM}$ and nRMSE$_{opt}$ almost exhibit similar trend with low ensemble nRMSE value of 1.51% for the HMM+ξ and 1.42% for HMM+GA+ξ.

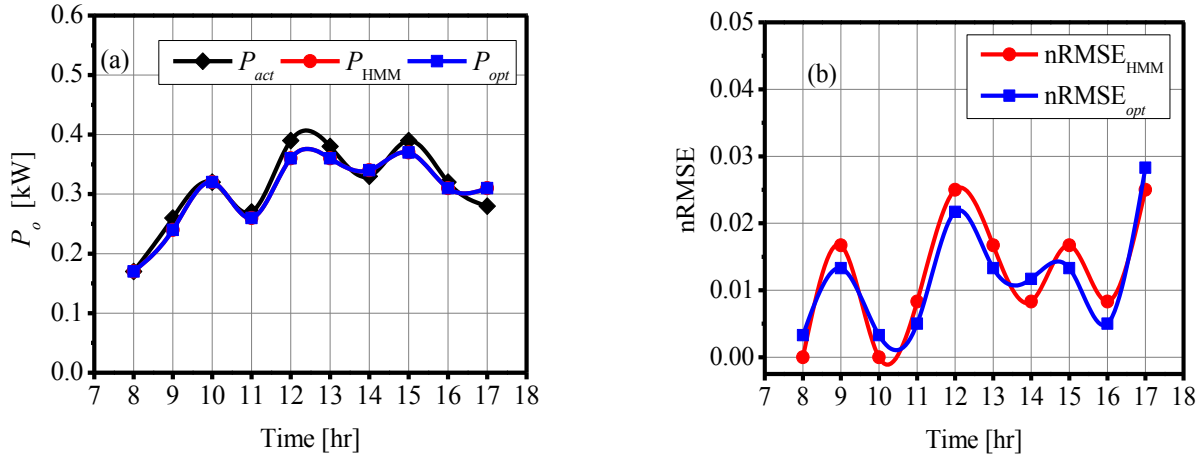

Fig. 10. P_o forecast and nRMSE of models 26.06.2018 using HMM+ξ and HMM+GA+ξ.

Table 2. Forecast model performance from March to June 2018

Date	Class	Models	nRMSE [%]		MAPE [%]	
			P_{HMM}	P_{opt}	P_{HMM}	P_{opt}
09.04.2018	CSD	HMM/HMM+GA	5.36	2.55	11.17	4.94
15.04.2018	CSD	HMM/HMM+GA	6.27	1.51	13.43	3.09
23.04.2018	CSD	HMM/HMM+GA	6.33	1.77	13.40	4.20
30.04.2018	CD	HMM+ξ/HMM+GA+ξ	5.61	4.29	15.64	12.33
25.03.2018	CD	HMM+ξ/HMM+GA+ξ	5.11	2.42	12.95	8.55
26.06.2018	CD	HMM+ξ/HMM+GA+ξ	1.51	1.42	4.63	4.52
Average			5.03	2.33	11.87	6.27

The model performance of the HMM and GA-optimized HMM with or without ξ on the hour-ahead forecasting of P_o of the PV system under different conditions of G_s (CSD or CD) are summarized in Table 2. For the days considered in the validation process, the reliability of the HMM and GA-integrated HMM is indicated by ensemble nRMSE and MAPE. It can be observed that both nRMSE and MAPE reduced when GA is integrated with HMM, corresponding to the class of day under CSD consideration. This reflects PV power forecasting with GA-integrated HMM has a higher P_o prediction capability, as the results of the optimized forecast parameters. In the case of instantaneous G_s on CD consideration, the data analytics stipulated the decision support tool for the application of ξ-adapted HMM and HMM+GA. It was deduced that if $|\overline{\Delta G_s}|$ is more than 128% in the morning, ξ in the range of 0.33 - 0.41 is acceptable. On the other hand, if $|\overline{\Delta G_s}|$ in the evening time exceeds 90%; appropriate ξ is in the range of 0.24 - 0.35. The use of ξ for the days in which fluctuation in G_s is pronounced, further improves the accuracy of forecast as expressed in percentage of nRMSE and MAPE. The HMM with or without ξ presents the average nRMSE and MAPE larger than HMM+GA with or without ξ. In addition, the average nRMSE and MAPE of HMM+GA with or without ξ is 2.33% and 6.27%. Therefore, the integration of GA and ξ into HMM are able to improve the forecasting accuracy of the hour-ahead P_o of the PV system as a result of the optimized forecast parameters.

Comparing with previous studies, Z. Zhong et al. presented a short-term day-ahead PV power generation volume based on multivariable Grey theory model improved with Particle Swarm Optimization (PSO); indicating that the model verification with PSO yields Mean Relative Error (MRE) decreasing from 7.14% to 3.53%, which corresponds to about 51% reduction [16]. However, the technique enunciated in this study gives a percentage reduction in nRMSE of about 54%. W. Zhang et al. articulated a 10 minute-ahead PV P_o forecasting using fuzzy clustering analysis with SVR model and reported an average nRMSE of 5.55% [18]. In contrast, our model presents an average nRMSE of 2.33%.

A. Lahouar et al. proposed a short-term day-ahead PV P_o forecast based on random forests using bagging algorithm with and without former information on the solar irradiance, and the authors reported a MAPE of 28.97% in the month of April [8]. A multivariate ensemble framework for seasonal one day and week-ahead PV P_o forecast using Autoregressive predicator, Particle Swarm Optimized-Radial Basis Function (PSO-RBF) network predicator and Particle Swarm Optimized-Feed-forward Neural Network (PSO-FNN) predictor presented an nRMSE of 9.55% for CSD and 9.51% for CD in the spring season [27]. With the model proposed in this study, the maximum MAPE in the month of April is 12.33% and the maximum nRMSEs are 6.33% and 5.61% for CSD and CD, respectively.

In the present study, therefore, GA-optimized HMM with or without ξ has been considered a good model for the hour-ahead P_o forecasting of the PV system. This model can be deployed by power system owners and grid operators, offering them some benefits including power quality, load drop or gain, reduced reserve costs, pricing-ahead of energy, better energy planning and management. In practical application, this forecast model can be suitably applied in locations or area whose weather pattern is similar to Thailand's. However, in case the nature of meteorological parameters follows a different pattern, the model retraining may be required using at least 6 months of historical data from the PV power plant.

4. Conclusion

In this study, the hour-ahead P_o forecasting of the PV system based on ordinary model (HMM) and optimized model (HMM+GA) together with or without correction factor (ξ) has been proposed. On the class of the day under CSD consideration, HMM+GA is able to predict the P_o with high forecasting accuracy. In a typical CD consideration, ξ is required to adapt HMM+GA when $|\overline{\Delta G_s}| \geq 128\%$ in the morning and/or $|\overline{\Delta G_s}| \geq 90\%$ in the evening time. The proposed optimized model presents higher accuracy than the ordinary model in all the days considered. With its average nRMSE and MAPE computed to be 2.33% and 6.27% respectively, GA-optimized HMM with or without ξ has been considered a good approach to hour-ahead forecasting of PV power output.

Acknowledgements

The authors express sincere gratitude to the Thailand International Cooperation Agency (TICA), Ministry of Foreign Affairs; Thailand for giving the scholarship in the Master degree program to Mr Victor Eniola from Nigeria. Also, the authors appreciate Naresuan University and the School of Renewable Energy and Smart Grid Technology (SGtech), Phitsanulok, Thailand for their kind cooperation.

References

[1] R. Al-Hajj, A. Assi, and M.M. Fouad. "A predictive evaluation of global solar radiation using recurrent neural models and weather data", 2017 IEEE 6th International Conference on Renewable Energy Research and Applications (ICRERA), DOI: 10.1109/ICRERA.2017.8191265, p. 195-199, 2017.

[2] A. Alzahrani, P. Shamsi, M. Ferdowsi, and C. Dagli. "Solar irradiance forecasting using deep recurrent neural networks", 2017 IEEE 6th International Conference on Renewable Energy Research and Applications (ICRERA), DOI: 10.1109/ICRERA.2017.8191206, p. 988-994, 2017.

[3] H. Wang, H. Yi, J. Peng, G. Wang, Y. Liu, H. Jiang, and W. Liu, "Deterministic and probabilistic forecasting of photovoltaic power based on deep convolutional neural network", Energy Conversion and Management, 153: p. 409-422, 2017.

[4] M. Yesilbudak, M. Çolak, and R. Bayindir. "A review of data mining and solar power prediction", 2016 IEEE International Conference on Renewable Energy Research and Applications (ICRERA), DOI: 10.1109/ICRERA.2016.7884507, p. 1117-1121, 2016.

[5] M. Yesilbudak, M. Colak, R. Bayindir, and H.I. Bulbul. "Very-short term modeling of global solar radiation and air temperature data using curve fitting methods", 2017 IEEE 6th International Conference on Renewable Energy Research and Applications (ICRERA), DOI: 10.1109/ICRERA.2017.8191233, p. 1144-1148, 2017.

[6] M. Omar, A. Dolara, G. Magistrati, M. Mussetta, E. Ogliari, and F. Viola. "Day-ahead forecasting for photovoltaic power using artificial neural networks ensembles", 2016 IEEE International Conference on Renewable Energy Research and Applications (ICRERA), DOI: 10.1109/ICRERA.2016.7884513, p. 1152-1157, 2016.

[7] M. Yesilbudak, M. Colak, and R. Bayindir, "What are the Current Status and Future Prospects in Solar Irradiance and Solar Power Forecasting?", International Journal of Renewable Energy Research, 8(1), 2018.

[8] A. Lahouar, A. Mejri, and J.B.H. Slama. "Importance based selection method for day-ahead photovoltaic power forecast using random forests", 2017 International Conference on Green Energy Conversion Systems (GECS), DOI: 10.1109/GECS.2017.8066171, p. 1-7, 2017.

[9] E. Ogliari, A. Dolara, G. Manzolini, and S. Leva, "Physical and hybrid methods comparison for the day

ahead PV output power forecast", Renewable Energy, 113: p. 11-21, 2017.

[10] Y. Liu, L. Ye, H. Qin, X. Hong, J. Ye, and X. Yin, "Monthly streamflow forecasting based on hidden Markov model and Gaussian Mixture Regression", Journal of Hydrology, 561: p. 146-159, 2018.

[11] L.R. Rabiner, "A tutorial on hidden Markov models and selected applications in speech recognition", Proceedings of the IEEE, 77(2): p. 257-286, 1989.

[12] S. Leva, A. Dolara, F. Grimaccia, M. Mussetta, and E. Ogliari, "Analysis and validation of 24 hours ahead neural network forecasting of photovoltaic output power", Mathematics and Computers in Simulation, 131: p. 88-100, 2017.

[13] V. Sharma, D. Yang, W. Walsh, and T. Reindl, "Short term solar irradiance forecasting using a mixed wavelet neural network", Renewable Energy, 90: p. 481-492, 2016.

[14] Y. Yang and L. Dong. "Short-Term PV Generation System Direct Power Prediction Model on Wavelet Neural Network and Weather Type Clustering", 5th International Conference on Intelligent Human-Machine Systems and Cybernetics, DOI: 10.1109/IHMSC.2013.56, p. 207-211, 2013.

[15] Y.z. Li, R. Luan, and J.c. Niu. "Forecast of power generation for grid-connected photovoltaic system based on grey model and Markov chain", 2008 3rd IEEE Conference on Industrial Electronics and Applications, DOI: 10.1109/ICIEA.2008.4582816, p. 1729-1733, 2008.

[16] Z. Zhong, C. Yang, W. Cao, and C. Yan, "Short-Term Photovoltaic Power Generation Forecasting Based on Multivariable Grey Theory Model with Parameter Optimization", Mathematical Problems in Engineering, 2017: p. 9, 2017.

[17] F. Barbieri, S. Rajakaruna, and A. Ghosh, "Very short-term photovoltaic power forecasting with cloud modeling: A review", Renewable and Sustainable Energy Reviews, 75: p. 242-263, 2017.

[18] W. Zhang, X. Zheng, X.S.J. Geng, Q.N.J. Li, and C. Bao. "Short-term photovoltaic output forecasting based on correlation of meteorological data", IEEE Conference on Energy Internet and Energy System Integration (EI2), DOI: 10.1109/EI2.2017.8245285, p. 1-5, 2017.

[19] L. Fen, L. Chunyang, Y. Yong, Y. Quanquan, Z. Jinbin, and W. Lijuan, "Short-term photovoltaic power probability forecasting based on OLPP-GPR and modified clearness index", The Journal of Engineering, 2017(13): p. 1625-1628, 2017.

[20] M.G. De Giorgi, P.M. Congedo, M. Malvoni, and D. Laforgia, "Error analysis of hybrid photovoltaic power forecasting models: A case study of mediterranean climate", Energy Conversion and Management, 100: p. 117-130, 2015.

[21] A.T. Eseye, J. Zhang, and D. Zheng, "Short-term photovoltaic solar power forecasting using a hybrid Wavelet-PSO-SVM model based on SCADA and Meteorological information", Renewable Energy, 118: p. 357-367, 2018.

[22] J. Li, J.K. Ward, J. Tong, L. Collins, and G. Platt, "Machine learning for solar irradiance forecasting of photovoltaic system", Renewable Energy, 90: p. 542-553, 2016.

[23] S. Dubey, J.N. Sarvaiya, and B. Seshadri, "Temperature Dependent Photovoltaic (PV) Efficiency and Its Effect on PV Production in the World – A Review", Energy Procedia, 33: p. 311-321, 2013.

[24] N. Savvakis and T. Tsoutsos, "Performance assessment of a thin film photovoltaic system under actual Mediterranean climate conditions in the island of Crete", Energy, 90: p. 1435-1455, 2015.

[25] J. Joshi, K. Tankeshwar, and S. Srivastava, "Hidden Markov Model for Quantitative Prediction of Snowfall and Analysis of Hazardous Snowfall Events over Indian Himalaya", Journal of Earth System Science: p. 126: 033, 2017.

[26] J. Wang, R. Ran, and Y. Zhou, "A Short-Term Photovoltaic Power Prediction Model Based on an FOS-ELM Algorithm", Applied Sciences, 7: p. 423, 2017.

[27] M.Q. Raza, M. Nadarajah, and C. Ekanayake. "A multivariate ensemble framework for short term solar photovoltaic output power forecast", 2017 IEEE Power & Energy Society General Meeting, DOI: 10.1109/PESGM.2017.8274676, p. 1-5, 2017.